

# Optical properties of metal phthalocyanines

Priyanka Singh · N. M. Ravindra

Received: 1 October 2009 / Accepted: 5 April 2010 / Published online: 20 April 2010  
© Springer Science+Business Media, LLC 2010

**Abstract** In this study, optical properties of phthalocyanines of five metals, i.e., cobalt, nickel, iron, copper, and manganese, have been discussed in the energy ( $E$ ) range of 1.5–4.1 eV. Utilizing the available data of refractive index ( $n$ ) and extinction coefficient ( $k$ ) of these materials in the literature, the related optical properties such as the real ( $\epsilon_1$ ), imaginary ( $\epsilon_2$ ) parts of the complex dielectric constant ( $\epsilon$ ), and reflectivity ( $R$ ) are calculated. Interpretations for the energies corresponding to the peaks in  $\epsilon_2$  are explained in terms of the Penn gap ( $E_P$ ). High-frequency dielectric constant ( $\epsilon_\infty$ ) values corresponding to four models, i.e., the conventional Lorentz model, modified Lorentz model, relaxed Lorentz model, and the dual Lorentz model are used to determine  $E_P$ . It is found that the  $E_P$  values corresponding to the conventional and dual Lorentz models are in good agreement with the average of energy peaks in the  $R$ - $E$  and the  $\epsilon_2$ - $E$  spectra. The oscillator energy ( $E_0$ ) and the dispersion energy ( $E_d$ ) of these materials have been determined utilizing the Wemple–DiDomenico model. The calculated values of (a)  $E_0$  are generally in good agreement with the Penn gap  $E_P$ , the average of the energy peaks in the  $R$ - $E$  and the  $\epsilon_2$ - $E$  spectra and (b)  $E_d$  are comparable to those in the literature for CoPc and NiPc.

## Introduction

Phthalocyanines (Pcs) are macrocyclic compounds, and have attracted much attention due to their unique physical and chemical properties [1, 2]. In recent years, the

applications of metal phthalocyanine (MPc) complexes have been expanded to include light emitting diodes [3], optical limiting devices [4, 5], liquid crystals [6], gas sensors [7–9], bio-sensors [10–12], photovoltaic cells [13, 14], photodynamic therapy [15–18], and in semiconductor materials [19, 20]. A mushroom-based cobalt phthalocyanine biosensor has been utilized for the determination of phenolic compounds [10]. A copper phthalocyanine chemoresistor has been used as a transducer in biosensing application [11]. It is important to note here that cobalt and nickel phthalocyanines may behave as carcinogens [21].

One of the most promising fields is the use of phthalocyanine derivatives as photosensitizers for photodynamic therapy (PDT), an emerging technology for treating a large variety of pathologies such as psoriasis, tumor, cancer, dysplastic, and infectious diseases [17]. While lipophilic phthalocyanine derivatives are reported to have a higher tumor affinity, associated with cutaneous phototoxicity [18], water soluble phthalocyanines are considered to be the best targets for a new generation of photosensitizers [16]. In a typical treatment of PDT, the patient receives an injection of the photosensitizer and waits for a short duration. This waiting period allows the photosensitizer to enrich in the tumor. Then, the tumor is illuminated by light with an appropriate wavelength. The excited photosensitizer causes a series of photodynamic reactions and destroys the tumor cell. Compared with traditional treatments such as surgery, iatrochemistry, and radiotherapy, the advantage of PDT is that it can destroy tumor selectively and does not harm the normal surrounding tissues seriously [1, 16]. During PDT, singlet oxygen is the predominant cytotoxic agent that is produced. This occurs when the photosensitizer undergoes electronic excitation from a ground singlet state to an excited singlet state; the excited singlet state is highly unstable, and rapidly

P. Singh · N. M. Ravindra (✉)  
Department of Physics, New Jersey Institute of Technology,  
Newark, NJ 07102, USA  
e-mail: nmravindra@gmail.com

undergoes intersystem crossing to a longer-living excited triplet state. One of the few chemical species present in the tissue is triplet state oxygen. When the photosensitizer and an oxygen molecule are in proximity, energy transfer takes place. It is this energy that is responsible for the spin inversion in molecular oxygen [16]. Therefore, in order to be used for PDT, a phthalocyanine must have a high yield of triplet state (and a concomitant high yield of singlet oxygen) and a long wavelength absorption in the red region of the visible spectrum [22]. MPc complexes have been proved as highly promising photosensitizers for PDT due to their intense absorption in the red region of the visible light. Complex structures of phthalocyanine with transition metals give short triplet lifetimes to these dyes. Closed shell and diamagnetic ions, such as  $Zn^{2+}$ ,  $Al^{3+}$ , and  $Si^{4+}$ , provide phthalocyanine complexes with both high triplet yields and long lifetimes [15, 16]. Therefore, the optical properties of these MPcs are the key to their recent success within PDT.

Furthermore, in order to improve the overall performance of electronic, opto-electronic, gas- sensing, and bio-sensing devices, based on phthalocyanines, it is important to study the electronic and optical properties of MPcs to understand the complex nature of their excited states. Moreover, determination of optical properties such as refractive index ( $n$ ), extinction coefficient ( $k$ ), and dielectric constant ( $\epsilon = \epsilon_1 + i\epsilon_2$ ) are interesting for many applications of MPcs [23]. In view of its numerous applications, the optical properties phthalocyanines of five metals, cobalt (Co), nickel (Ni), copper (Cu), iron (Fe), and manganese (Mn), have been discussed in this article. In particular, we discuss the spectral dependence of the optical constants;  $n$ ,  $k$ ,  $\epsilon_1$ ,  $\epsilon_2$ , and reflectivity ( $R$ ) of these MPcs. The real and imaginary parts of the optical dielectric constant,  $\epsilon_1$  and  $\epsilon_2$ , are calculated using the phenomenological expressions:

$$\epsilon_1 = n^2 - k^2 \quad (1)$$

$$\epsilon_2 = 2nk \quad (2)$$

The reflectivity has been determined using the following expression:

$$R = \frac{(n-1)^2 + k^2}{(n+1)^2 + k^2} \quad (3)$$

$\epsilon_1$ ,  $\epsilon_2$ ,  $R$ ,  $n$ , and  $k$  are functions of the photon energy,  $E$ .

## Results and discussion

The analysis of the optical properties of metal phthalocyanines, i.e., CoPc, NiPc, CuPc, FePc, and MnPc, in this study, are based on the results of the energy dependence of the fundamental optical constants,  $n$  and  $k$ , in the literature

[24–26]. The data of the optical properties, considered in this study, are those of thin films of CoPc, NiPc, CuPc, MnPc, and FePc deposited on glass substrates [24–26]. The thickness range of CoPc, NiPc, and FePc films is  $\sim 80$ – $100$  nm [24], CuPc is  $\sim 170$  nm [25], and MnPc is  $\sim 204$ – $630$  nm [26].

Figure 1 shows the variations in  $n$ ,  $k$ ,  $\epsilon_1$ ,  $\epsilon_2$  and  $R$  with  $E$  for CoPc, NiPc, CuPc, MnPc, and FePc, in the spectral range of 1.5–4.1 eV (300–800 nm). It is evident from Fig. 1 that  $n$ ,  $k$ ,  $\epsilon_1$ ,  $\epsilon_2$  and  $R$  vary significantly with  $E$ . As can be seen in Fig. 1,  $\epsilon_2$ - $E$  and  $R$ - $E$  spectra of CoPc, NiPc, and CuPc exhibit two sharp peaks and one broad peak; however, the corresponding spectra for FePc and MnPc exhibit one sharp peak and one broad peak. The energies corresponding to these peaks in the  $R$ - $E$  and  $\epsilon_2$ - $E$  spectra of Fig. 1 are listed in Table 1. For the  $\epsilon_2$ - $E$  spectra, these energies,  $E_1$ ,  $E_2$ , and  $E_3$  in eV, respectively, are: (a) 1.81, 1.99, and 3.75 for CoPc (b) 1.82, 1.98, and 3.57 for NiPc, and (c) 1.80, 2.02, and 3.52 for CuPc. However,  $E_1$  and  $E_3$  for (d) FePc, respectively, are 1.94 and 3.54 eV, and for (e) MnPc, 1.70 and 3.45 eV. For  $R$ - $E$  spectra, these energies,  $E_{R1}$ ,  $E_{R2}$ , and  $E_{R3}$  in eV, respectively, are: (a) 1.76, 1.99, and 3.63 for CoPc, (b) 1.77, 1.98, and 3.54 for NiPc and (c) 1.73, 1.96, and 3.30 for CuPc. However,  $E_{R1}$  and  $E_{R3}$  for (d) FePc are 1.71 and 3.5 eV and for (e) MnPc, 1.71 and 2.81 eV. In addition to these peaks, FePc and MnPc also exhibit a small peak and shoulder in both the spectra and the corresponding energy values are listed in Table 1 in parentheses. In the  $\epsilon_2$ - $E$  spectra, FePc exhibits a small peak at 3.75 eV and a shoulder at 1.76 eV and MnPc exhibits a small peak at 2.31 eV and a shoulder at 1.97 eV. In  $R$ - $E$  spectra, FePc exhibits a small peak at 3.74 eV and a shoulder at 1.9 eV and MnPc exhibits a shoulder at 1.97 eV.

## Application of Penn model

The reflectivity spectra or the  $\epsilon_2$ - $E$  spectra of a given material are described by its band structure. Conceptually, the intensity maximum in  $\epsilon_2$  (or  $R$ ) represents a maximum number in the optically induced electronic transitions in the material [27]. The energy corresponding to the peak in  $\epsilon_2$  (or  $R$ ) should, therefore, correspond to band-to-band energy difference or a band gap. Since this is macroscopic gap [28], it should be related to the high-frequency dielectric constant  $\epsilon_\infty$  ( $\approx n^2$ ).

Several models have been proposed [28, 29] to interpret the frequency and wave vector dependence of the dielectric function. However, all these models have been proposed for elemental semiconductors. Extrapolations of the applicability of these models to amorphous semiconductors [30], narrow and wide-gap materials including alkali

**Fig. 1** Variation of  $n$ ,  $k$ ,  $\epsilon_1$ ,  $\epsilon_2$ , and  $R$  as a function of photon energy for CoPc [24], CuPc [25], FePc [24], and MnPc [26]

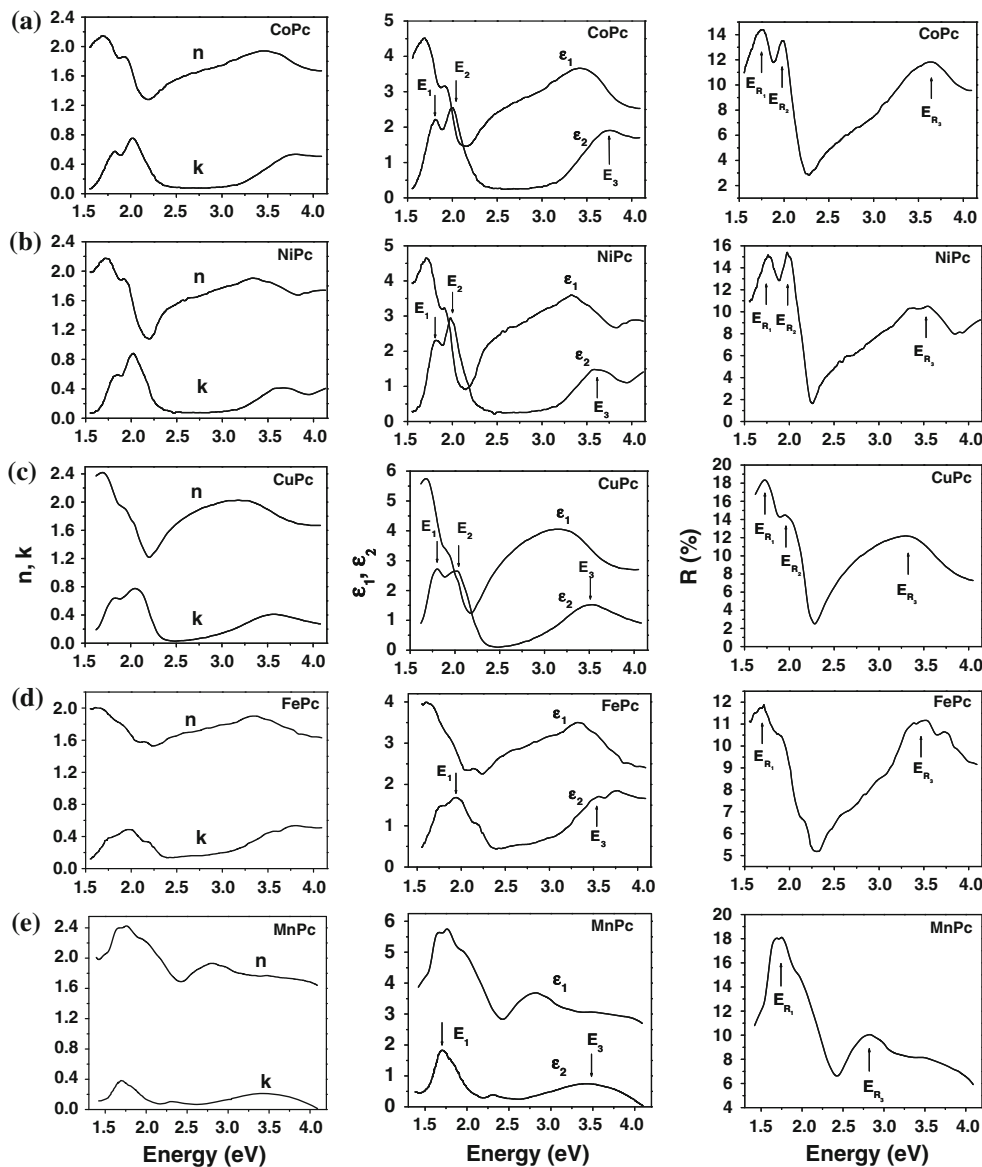


**Table 1** Reflectivity and  $\epsilon_2$  data of cobalt phthalocyanine, nickel phthalocyanine, iron phthalocyanine, copper phthalocyanine, and manganese phthalocyanine

MPc	$E_1$ (eV)	$E_2$ (eV)	$E_3$ (eV)	$E_{R1}$ (eV)	$E_{R2}$ (eV)	$E_{R3}$ (eV)
CoPc	1.81	1.99	3.75	1.76	1.99	3.63
NiPc	1.82	1.98	3.57	1.77	1.98	3.54
CuPc	1.80	2.02	3.52	1.73	1.96	3.3
FePc	1.94		3.54	1.71		3.5
			(3.75)			(3.74)
			(1.76)			(1.9)
MnPc	1.70		3.45	1.71		2.81
			(2.31)			(1.97)
			(1.97)			

halides [31, 32] have been carried out with reasonable success. Here, we demonstrate the applicability of the model to these five metal phthalocyanines.

For a model semiconductor,  $\epsilon_\infty$  is given by [28]:

$$\epsilon_\infty = 1 + (\hbar\omega_p/E_p)^2 \left[ 1 - (E_p/4E_F) + \frac{1}{3}(E_p/4E_F)^2 \right] \quad (4)$$

or

$$1/E_p = 1/8E_F + \left[ (\epsilon_\infty - 1)/(\hbar\omega_p)^2 - \frac{1}{3}(1/8E_F)^2 \right]^{1/2} \quad (5)$$

where, the valance electron plasmon energy  $\hbar\omega_p$  is given by [33]:

$$\hbar\omega_p = 28.8(N_{\text{eff}}\rho/M)^{1/2} \quad (6)$$

In Eqs. 4 and 5,  $E_p$  is the Penn gap [28] or the macroscopic gap accounting for all the possible optically induced electronic transitions in the material, and  $E_F$  is the Fermi energy evaluated using the relation [32]:

$$E_F = 0.2947(\hbar\omega_p)^{4/3} \quad (7)$$

In Eq. 6,  $N_{\text{eff}}$  is the number of valence electrons per atom and is determined using the expression described elsewhere [34],  $M$  is the molecular weight, and  $\rho$  is the density of the metal phthalocyanine [2]. The values of  $\varepsilon_\infty$  for CoPc, NiPc, CuPc, and FePc are available in the literature [24]. In reference [24], the optical functions were determined by fitting the optical data obtained by spectroscopic ellipsometry (SE) measurements. The data were fitted with the conventional Lorentz model (CLM), modified Lorentz model (MLM), relaxed Lorentz model (RLM), and the dual Lorentz model (DLM). These model calculations have led to four values of  $\varepsilon_\infty$  [24]. These corresponding  $\varepsilon_\infty$  values have been used to calculate  $E_p$ . In CLM, the dielectric function ( $\varepsilon = \varepsilon_1 + i\varepsilon_2$ ) is given by [25, 35, 36]:

$$\varepsilon(\omega) = \varepsilon_\infty + \sum_j \frac{F_j}{\omega_j^2 - \omega^2 + i\Gamma_j\omega} \quad (8)$$

where,  $j$  is the total number of Lorentzian oscillators, and  $\omega_j$ ,  $F_j$ , and  $\Gamma_j$  are the peak frequency, strength, and broadening of the  $j$ th oscillator, respectively.

The dielectric function in MLM is given by the following Eq. [25]:

$$\varepsilon(\omega) = \varepsilon_\infty + \sum_j \frac{F_j}{\omega_j^2 - \omega^2 - i\Gamma'_j\omega} \quad (9)$$

where,  $j$  is the total number of Lorentzian oscillators, and  $\omega_j$ ,  $F_j$ , and  $\Gamma'_j$  are the peak frequency, strength, and broadening of the  $j$ th oscillator, respectively. Unlike CLM, where the width,  $\Gamma$ , is a constant, in MLM,  $\Gamma'_j$  is a function of frequency given by [25],

$$\Gamma'_j(\omega) = \Gamma_j(\omega) \exp\left[-\alpha_j\left(\frac{|\hbar\omega| - \hbar\omega_j}{\Gamma_j}\right)\right] \quad (10)$$

where,  $\alpha_j$  is the broadening factor of  $j$ th oscillator. If  $\alpha_j = 0$ , then the  $j$ th oscillator is a Lorentz oscillator. When  $\alpha_j \sim 0.2$ , then the  $j$ th oscillator is a Gaussian-like oscillator. The dielectric function in RLM is given by [35, 36],

$$\varepsilon(\omega) = \varepsilon_\infty + \sum_j \frac{F_j e^{i\beta_j}}{\omega_j^2 - \omega^2 - i\Gamma'_j\omega} \quad (11)$$

where,  $j$  is the total number of Lorentzian oscillators, and  $\omega_j$ ,  $F_j$ ,  $\Gamma'_j$ , and  $\beta_j$  are the peak frequency, strength,

broadening, and phase factor of the  $j$ th oscillator, respectively. The DLM is based on the classical Lorentz model [24]. The parameter  $\Gamma$  in the CLM represents the width of the oscillator. In DLM, each oscillator has two  $\Gamma$  values, one for the lower energy side of the peak and other one for the higher side. For each oscillator, the dielectric constant is assumed as below:

$$\varepsilon(\omega) = \varepsilon_\infty + \begin{cases} \frac{F}{\omega^2 - \omega_0^2 + i\Gamma_1\omega} & \omega < \omega_0 \\ \frac{F\Gamma_2}{\omega^2 - \omega_0^2 + i\Gamma_2\omega} & \omega \geq \omega_0 \end{cases} \quad (12)$$

where,  $\omega_0$  is the oscillator frequency,  $F$  is the oscillator strength,  $\Gamma_1$  and  $\Gamma_2$  are the two widths.

The results of these calculations are presented in Table 2. Table 2 also lists the values of band gap energy ( $E_g$ ) for CoPc [37], NiPc [38], CuPc [38], FePc [39], and MnPc [26]. These values of  $E_g$  are determined from  $\alpha^2$  vs.  $h\nu$  graph [26, 37–39]. The values of Penn gap,  $E_p$ , listed in Table 2, have been determined using Eq. 5 for the corresponding values of  $\varepsilon_\infty$ . In Table 2,  $\bar{E}_R$  represents the average of energies  $E_{R1}$ ,  $E_{R2}$ , and  $E_{R3}$  in the  $R$ - $E$  spectra, and  $\bar{E}$  represents the average of energies  $E_1$ ,  $E_2$ , and  $E_3$  in the  $\varepsilon_2$ - $E$  spectra for CoPc, NiPc, and CuPc. However, for FePc and MnPc,  $\bar{E}_R$  represents the average of energies  $E_{R1}$  and  $E_{R3}$  in  $R$ - $E$  spectra, and  $\bar{E}$  represents average of energies  $E_1$  and  $E_3$  in the  $\varepsilon_2$ - $E$  spectra. The parenthesis value of  $\bar{E}_R$  and  $\bar{E}$  for FePc and MnPc represent the average of these two peaks, one small peak and a shoulder in the corresponding spectra.

As can be seen from Table 2, (a) for CoPc, the four  $E_p$  values are obtained for four  $\varepsilon_\infty$  values corresponding to four models (CLM, RLM, DLM, and MLM), the value of  $\varepsilon_\infty$  is 1.6 for CLM and DLM and the corresponding value of  $E_p$  (2.54 eV) for this value is very close to  $\bar{E}$  and slightly differs with  $\bar{E}_R$ . However, for RLM ( $\varepsilon_\infty = 1.43$ ) and MLM ( $\varepsilon_\infty = 1.24$ ), the calculated values of  $E_p$  are higher than  $\bar{E}$  and  $\bar{E}_R$ . The two reported values of  $\varepsilon_\infty$  for CoPc thin films are mentioned in parentheses, where  $\varepsilon_\infty = 3.15$  corresponds to nanocrystalline CoPc film and  $\varepsilon_\infty = 3.56$  corresponds to CoPc thin films [40]. The calculated values of  $E_p$  (in parentheses) corresponding to these  $\varepsilon_\infty$  values are 1.53 and 1.42 eV and noticeably differ with  $\bar{E}$  and  $\bar{E}_R$ .

For (b) NiPc, the four  $E_p$  values are calculated for four models CLM ( $\varepsilon_\infty = 1.55$ ), RLM ( $\varepsilon_\infty = 1.49$ ), DLM ( $\varepsilon_\infty = 1.73$ ), and MLM ( $\varepsilon_\infty = 1.04$ ). The calculated value of  $E_p$  (2.41 eV) for DLM ( $\varepsilon_\infty = 1.73$ ) is approximately equal to  $\bar{E}_R$  and slightly differs with  $\bar{E}$ . However, for CLM and RLM, the obtained values of  $E_p$  are comparable to  $\bar{E}$  and  $\bar{E}_R$ , for MLM ( $\varepsilon_\infty = 1.24$ ), the calculated  $E_p$  (6.86 eV) is higher than  $\bar{E}$  and  $\bar{E}_R$ . El-Nahass et. al. [41] have reported a value of  $\varepsilon_\infty = 3.71$  for NiPc thin films. The

**Table 2** Properties of metal phthalocyanines (CoPc, NiPc, CuPc, FePc, and MnPc)

MPc	Chemical formula	Mol. wt. (M)	$\rho$ (g/cm <sup>3</sup> )	$E_g$ (eV)	$N_{\text{eff}}$	$\hbar\omega_p$	$E_F$ (eV)	Model	$\epsilon_\infty$	$E_P$ (eV)	$\bar{E}_R$ (eV)	$\bar{E}$ (eV)			
CoPc	C <sub>32</sub> H <sub>16</sub> N <sub>8</sub> Co	571	1.53	3.25 [37]	3.26	2.69	1.10	CLM	1.60	2.54	2.46	2.52			
								RLM	1.43	2.88					
								DLM	1.60	2.54					
								MLM	1.24	3.53					
									(3.15) [40]	(1.53)					
									(3.56) [40]	(1.42)					
					(3.28)	(2.70)	(1.11)		1.60	(2.55)					
NiPc	C <sub>32</sub> H <sub>16</sub> N <sub>8</sub> Ni	571	1.59	2.64 [38]	3.26	2.75	1.13	CLM	1.55	2.68	2.43	2.46			
								RLM	1.49	2.80					
								DLM	1.73	2.41					
								MLM	1.04	6.86					
									(3.71) [41]	(1.42)					
					(3.28)	(2.75)	(1.14)		1.73	(2.42)					
CuPc	C <sub>32</sub> H <sub>16</sub> N <sub>8</sub> Cu	576	1.61	2.71 [38]	3.26	2.75	1.14	CLM	1.39	3.05	2.33	2.45			
					(3.24)	(2.74)	(1.13)		1.39	(3.04)					
FePc	C <sub>32</sub> H <sub>16</sub> N <sub>8</sub> Fe	568	1.52	3.18 [39]	3.26	2.69	1.10	CLM	1.43	2.87	2.61	2.74			
								RLM	1.42	2.90	(2.71)	(2.75)			
								DLM	1.37	3.03					
								MLM	1.32	3.19					
									(3.28)	(2.70)	(1.11)				
MnPc	C <sub>32</sub> H <sub>16</sub> N <sub>8</sub> Mn	567	1.52	3.25 [26]	3.26	2.69	1.10	CLM	1.43	(2.88)					
					(3.28)	(2.70)	(1.11)	2.65	1.71	2.26	2.58				
					(3.28)	(2.70)	(1.11)			(1.71)	(2.16)	(2.36)			
					(3.30)	(2.71)	(1.11)			(1.71)					
					(3.32)	(2.72)	(1.12)			(1.72)					
					(3.33)	(2.72)	(1.12)			(1.73)					
					(3.35)	(2.73)	(1.12)			(1.73)					

$N_{\text{eff}}$  is the effective number of valence electrons per atom.  $\hbar\omega_p$  is the valence electron plasmon energy.  $E_F$  is the Fermi energy.  $\epsilon_\infty$  is the high-frequency dielectric constant.  $E_P$  is the Penn gap.  $\bar{E}$  is the average of all the energies corresponding to the peaks in  $\epsilon_2$ .  $E_g$  is the energy gap determined from  $\alpha^2$  vs.  $h\nu$  graph

corresponding  $E_P$  (in parentheses) is 1.42 eV which markedly differs with  $\bar{E}$  and  $\bar{E}_R$ .

For (c) CuPc, the realistic value of  $\epsilon_\infty$  is 1.39 for CLM; the other values of  $\epsilon_\infty$  (RLM-1.00, DLM-1.02 and MLM-1.00) [24] are not acceptable to calculate Penn gap in accordance with Eq. 5. The calculated value of  $E_P$  is higher than both  $\bar{E}$  and  $\bar{E}_R$ , however,  $E_P$  is more close to  $\bar{E}$ .

Also for (d) FePc, the four  $E_P$  values are obtained corresponding to four models, CLM ( $\epsilon_\infty = 1.43$ ), RLM ( $\epsilon_\infty = 1.42$ ), DLM ( $\epsilon_\infty = 1.37$ ), and MLM ( $\epsilon_\infty = 1.32$ ).  $E_P$  (2.87 eV), corresponding to CLM model is the closest value to  $\bar{E}$  and  $\bar{E}_R$ . For RLM, DLM, and MLM, the calculated  $E_P$  is higher than  $\bar{E}$  and  $\bar{E}_R$ .

For (d) MnPc, to the best of our knowledge, no previous data on  $\epsilon_\infty$  has been reported in the literature. Therefore,  $\epsilon_\infty$  ( $\sim 2.65$ ) is determined from the  $n$  versus  $k$  graph at high frequency at  $k$  ( $\approx 0$ ) [26]. The calculated value of  $E_P$

(1.71 eV) is lower than both  $\bar{E}$  and  $\bar{E}_R$  and differs considerably with  $\bar{E}$ .

It is important to note here that the closest  $E_P$  values 2.87 eV for FePc and 1.71 eV for MnPc, as discussed above are more close to their parenthesis values of  $\bar{E}$  (average of energies corresponding to  $E_1$ ,  $E_3$ , small peak, and shoulder) and  $\bar{E}_R$  (average of energies corresponding to  $E_{R1}$ ,  $E_{R3}$ , small peak, and shoulder), which shows the importance of Penn model in explaining the energy peaks in  $\epsilon_2$  - $E$  (or  $R$ - $E$ ) spectra. The noticeable difference in  $E_P$  and  $\bar{E}$  (or  $\bar{E}_R$ ) may be attributed to the fact that  $\rho$  and  $\epsilon_\infty$  mentioned in Table 2 for these MPcs do not pertain to the same MPcs on which the optical measurements were made. It is worthwhile to note here that such a procedure of comparing the calculated  $E_P$  with the average of the energies corresponding to the peak in  $\epsilon_2$  (or  $R$ ) was proposed by Phillips [42].



From the above results, it can be concluded that for CoPc, NiPc, CuPc, and FePc, the determined  $E_P$  values corresponding to CLM and DLM are in good accord with  $E_P$ ,  $\bar{E}$  and  $\bar{E}_R$ .

It should be noted that, in these five MPcs; CoPc, NiPc, FePc, CuPc, and MnPc, the central metals are transition metals which have their valence electrons in more than one shell. Based on their outer configurations, Co ( $4s^2 3d^7$ ), Ni ( $4s^2 3d^8$ ), and Fe ( $4s^2 3d^6$ ) may have 2 or 3 valence electrons. However, Cu ( $3d^{10} 4s^1$ ) may possess 1 or 2 valence electrons, and Mn ( $4s^2 3d^5$ ) may have variation in valence electrons from 2 to 7. Therefore, in Table 2, we have also evaluated the Penn gap incorporating the variation in  $N_{\text{eff}}$  (in parentheses, in Table 2), for the calculation of  $E_P$ ;  $\epsilon_\infty$  is chosen such that  $E_P$  value is closest to  $\bar{E}$  (or  $\bar{E}_R$ ) i.e., for CoPc, DLM, and CLM ( $\epsilon_\infty = 1.43$ ); for NiPc and DLM ( $\epsilon_\infty = 1.73$ ); for CuPc there is only one value, i.e.,  $\epsilon_\infty = 1.39$ ; and for FePc and CLM ( $\epsilon_\infty = 1.43$ ). The values of  $N_{\text{eff}}$  and  $E_P$  in parentheses for CoPc, NiPc, FePc, and CuPc represent the situation when Co, Ni, and Fe have 3 valence electrons, and Cu has 1 valence electron. However, for MnPc, the values in parentheses correspond to variation in valence electron from 3 to 7. It is to be noted that the calculated values of  $E_P$  for these MPcs incorporating the variation in valence electron contribution is in good agreement with  $\bar{E}$  (or  $\bar{E}_R$ ). For CoPc, NiPc, CuPc, and FePc, the value of  $E_P$  in parentheses is approximately equal to the previous  $E_P$  value; however, for MnPc, the calculated  $E_P$  increases slightly for valence electron values of 6 and 7. These results suggest that the valence electrons present in the central metal (Co, Ni, Fe, Cu, and Mn) contribute to the effective number of electrons in corresponding MPcs, and hence, to their optical spectra of  $\epsilon_2$ - $E$  (or R- $E$ ). The successful extrapolation of the application of Penn-like models to these metal phthalocyanines leads to interesting conclusions. An isotropic, nearly free electron model, such as the Penn model, seems to be valid for most materials, in explaining the energies corresponding to the peaks in the reflectivity spectra (or the  $\epsilon_2$ - $E$  spectra) and correlating these energies to the band structure of the material.

At this stage, it would be worthwhile to look into  $n$ - $\lambda$  (wavelength) variations. The well-known Wemple–DiDomenico model explains the  $n$ - $\lambda$  behavior in the form [43]:

$$n^2(E) - 1 = \frac{E_d E_0}{E_0^2 - E^2} \quad (13)$$

where,  $E_d$  is the dispersion energy and is proportional to the volume density of valance electrons involved in the transitions at  $E_0$ , and  $E_0$  is an average excitation energy or an interband transition energy (almost equal to Penn gap,

Ref. [30]) coinciding with the energy corresponding to  $\epsilon_2$  max in the  $\epsilon_2$ - $E$  spectra. Thus, a plot of  $1/(n^2 - 1)$  versus  $E^2$  will be a straight line and yields values of  $E_d$  and  $E_0$ . Such variations of  $n$  vs.  $E$  (as in Eq. 13) is valid for photon energies less than the band gap [44]. It was found that the dispersion energy,  $E_d$ , which is related to the interband transition strength, obeys an extraordinarily simple empirical relation for over 100 widely different ionic and covalent nonmetallic crystals and liquids [43].

Figure 2 shows a plot of  $1/(n^2 - 1)$  versus  $E^2$  for the five metal phthalocyanines, CoPc, NiPc, CuPc, FePc, and MnPc. It is observed that the plots are linear over the energy ranging from 1.8 eV to approximately 2.8 eV. The values of  $E_0$  and  $E_d$  are determined from the plot using the linear best fit parameters. These values are obtained from the intercepts and the slopes of the graphs of  $1/(n^2 - 1)$  versus  $E^2$  for CoPc, NiPc, FePc, CuPc, and MnPc. The values of  $E_d$  and  $E_0$  are summarized in Table 3 for CoPc, NiPc, CuPc, FePc, and MnPc. The respective values of  $E_d$  and  $E_0$  for these phthalocyanines, in eV, are as follows: (a) CoPc: 3.29 and 2.19; (b) NiPc: 4.06 and 2.36; (c) CuPc:

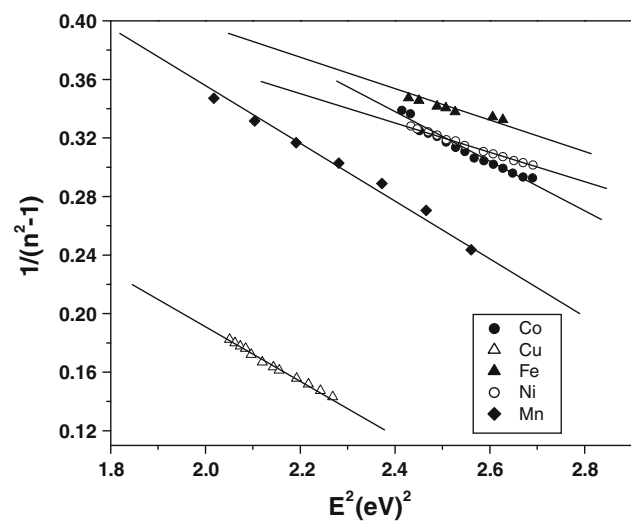


**Fig. 2** Plot of  $1/(n^2 - 1)$  versus  $E^2$  for CoPc, NiPc, FePc, CuPc, and MnPc

**Table 3** Wemple–DiDomenico parameters ( $E_d$  and  $E_0$ ) of metal phthalocyanines (CoPc, NiPc, CuPc, FePc, and MnPc)

MPc	$E_d$ (eV)	$E_0$ (eV)	Reported $E_d$ (eV)	Reported $E_0$ (eV)
CoPc	3.29	2.19	3.28 [40] 16.25 [40]	1.52 [40] 6.36 [40]
NiPc	4.06	2.36	3.50 [41]	8.06 [41]
CuPc	3.18	1.75	–	–
FePc	5.12	2.68	–	–
MnPc	2.77	1.98	–	–

3.18 and 1.75; (d) FePc: 5.12 and 2.68; and (e) MnPc: 2.77 and 1.98. El-Nahass et. al. [40, 41] have obtained the values of  $E_d$  and  $E_0$  for CoPc and NiPc thin films, and their graphs of  $1/(n^2 - 1)$  versus  $E^2$  were linear in the range of 0.60 eV to approximately 1.16 eV. The reported values of  $E_d$  and  $E_0$ , in eV, for CoPc thin films are  $E_d$ : 3.28 and 16.25 and  $E_0$ : 1.52 and 6.36, where the higher energy values correspond to CoPc thin films, and the lower energy values correspond to nanocrystalline CoPc films [40]. As can be seen from Table 3, the determined and reported values of  $E_d$  and  $E_0$  (corresponding to nanocrystalline CoPc film) are in good agreement. The determined  $E_0$  (2.19 eV) value is comparable to  $\bar{E}_R$  and  $\bar{E}$ .

The reported values of  $E_d$  and  $E_0$  for NiPc thin films are 3.5 and 8.06 eV, respectively [41]. As can be seen in Table 3, the determined value of  $E_d$ , for NiPc, is comparable to the reported value. However, the determined  $E_0$  value is lower than the reported value; this difference may be attributed to the difference in range of energies considered in the study and the fact that these represent thin films of metal Pcs on substrates. The determined  $E_0$  (2.36 eV) value is very close to  $\bar{E}_R$  and  $\bar{E}$ .

To the best of our knowledge, for CuPc, FePc, and MnPc, no previous data on  $E_d$  and  $E_0$  have been reported in the literature. In this study,  $E_0$  values for CuPc and MnPc are lower and noticeably differ with  $\bar{E}_R$  and  $\bar{E}$ . However, for FePc,  $E_0$  value is very close to  $\bar{E}_R$  and  $\bar{E}$ .

## Conclusions

Metal phthalocyanines have found applications in medicine and optoelectronics. The optical properties of five metal phthalocyanines, cobalt, nickel, iron, copper, and manganese, have been analyzed in this study. The available data of refractive index and extinction coefficient of these materials in the literature have been utilized to evaluate the relevant properties of these materials. Penn model leads to an explanation of the energies corresponding to the peaks in the  $\varepsilon_2$ - $E$  spectra and the  $R$ - $E$  spectra. High-frequency dielectric constant values corresponding to four models; conventional Lorentz model, modified Lorentz model, relaxed Lorentz model, and the dual Lorentz model were used to determine  $E_p$ .  $E_p$  values corresponding to CLM and DLM are in good agreement with the average of energy peaks in  $R$ - $E$  and  $\varepsilon_2$ - $E$  spectra. Oscillator energy,  $E_0$ , and the dispersion energy,  $E_d$ , have been determined using the Wemple–DiDomenico model. Interpretations for these energies have been sought in terms of the Penn model and have been compared with the results available in the literature.

## References

- Leznoff CC, Lever ABP (1996) Phthalocyanines: properties and applications, vol 4. VCH, New York
- Moser FH, Arthur Thomas L (1963) Phthalocyanine compounds. Reinhold Pub. Co, New York
- de la Torre G, Claessens CG, Torres T (2007) Chem Commun 2000
- Perry JW, Mansour K, Lee IYS et al (1996) Science 273:1533
- Zhang L, Wang L (2008) J Mater Sci 43(17):5692. doi:10.1007/s10853-008-2826-4
- Durmuş M, Yeşilot S, Ahsen V (2006) New J Chem 30:675
- Guillaud G, Simon J, Germain JP (1998) Coord Chem Rev 180:1433
- Fernandes AN, Richardson TH (2008) J Mater Sci 43(4):1305. doi:10.1007/s10853-007-2184-7
- Alarjah M, Paniwnyk L, Peterson IR, Lorimer JP, Walton DJ (2009) J Mater Sci 44(16):4246. doi:10.1007/s10853-009-3593-6
- Ozsoz M, Erdem A, Kilinc E, Gokgunec L (1996) Electroanalysis 8:147
- Sergeyeva TA, Lavrik NV, Rachkov AE, Kazantseva ZI, El'skaya AV (1998) Biosens Bioelectron 13:359
- Ravindra NM, Prodan C, Fnu S, Padron I, Sikha SK (2007) JOM 54:37
- Pakhomov GL, Pakhomov LG, Travkin VV et al (2010) J Mater Sci 45(7):1854. doi:10.1007/s10853-009-4169-1
- Guldi DM, Gouloumis A, Vazquez P, Torres T (2002) Chem-Commun 2056
- Bonnett R (1995) Chem Soc Rev 24:19
- Moser JG (1998) Photodynamic tumor therapy-2nd and 3rd generation photosensitizers. Harwood academic publishers, Amsterdam
- Oschner MJ (1997) Photochem Photobiol B: Biol 39:1
- Jori G (1996) J Photochem Photobiol B: Biol 36:87
- Gaffo L, Cordeiro MR, Freitas AR et al (2010) J Mater Sci 45(5):1366. doi:10.1007/s10853-009-4094-3
- Roy MS, Balraju P, Deol YS et al (2008) J Mater Sci 43(16):5551. doi:10.1007/s10853-008-2822-8
- Known and suspected carcinogens. Theoretical Chemistry Laboratory, Oxford University. <http://msds.chem.ox.ac.uk/carcinogens.html>. Accessed 30 Oct 2009
- Yarmush ML, Thorpe WP, Strong L et al (1993) Crit Rev Therapeut Drug Carrier Syst 10:197
- Heavens OS (1991) Optical properties of thin solid films. Dover, New York
- Liu ZT, Kwok HS, Djuricic AB (2004) J Phys D: Appl Phys 37:678
- Djuricic AB, Kwong CY, Lau TW et al (2002) Opt Commun 205:155
- Rajesh KR, Menon CS (2005) Eur Phys J B 47:171
- Ravindra NM, Weeks RA, Kinser DL (1987) Phys Rev B 36:6132
- Penn DR (1962) Phys Rev 128:2093
- Breckenridge RA, Shaw RW Jr, Sher A (1974) Phys Rev B10:2483
- Ravindra NM, Narayan J (1986) J Appl Phys 60:1139
- Van Vechten JA (1969) Phys Rev 182:891
- Kumar A, Ravindra NM (1982) Phys Rev B 25:2889
- Jackson JD (1978) Classical electrodynamics. Wiley, New York
- Lyle RE, Lyle GG (1978) Cell Mol Life Sci 34:1653
- Arwin H, Mårtensson J, Jansson R (1992) Appl Opt 31:6707
- Mårtensson J, Arwin H (1991) Thin Solid Films 205:252
- Joseph B, Menon CS (2008) E-J Chem 5:86
- Varghese AC, Menon CS (2005) Central Eur J Phys 3(1):8
- Seoudi R, El-Bahy GS, El Sayed ZA (2006) Opt Mater 29:304

40. El-Nahass MM, Farag AAM, Atta AA (2009) *Synthetic Metals* 159:589
41. El-Nahass MM, Farag AAM, Abd El-Rahman KF, Darwish AAA (2005) *Opt Laser Technol* 37:513
42. Phillips JC (1973) *Bonds and bands in semiconductors*. Academic, New York
43. Wemple SH, DiDomenico MD Jr (1971) *Phys Rev B* 3:1338
44. Ravindra NM, Narayan J (1987) *J Appl Phys* 61:2017